SYNTHESIS AND CHARACTERIZATION OF ZnO NANO-PARTICLES

Submitted *by*

Jayanta Kumar Behera

In partial fulfillment for the award of the Degree of

MASTER OF SCIENCE

IN

PHYSICS

UNDER THE ESTEEMED GUIDANCE OF

Dr. Dillip Kumar Bisoyi

DEPARTMENT OF PHYSICS

NATIONAL INSTITUTE OF TECHNOLOGY,

ROURKELA-769008, ORISSA, INDIA.

National Institute of Technology,

Rourkela

CERTIFICATE

This is to certify that the thesis entitled **"Synthesis and Characterization of ZnO nanoparticles"** is submitted by **Mr. JAYANTA KUMAR BEHERA**, (Roll NO- **407PH102**) to this Institute in partial fulfillment of the requirement for the award of the degree of Master of Science in **Department Physics,** is a bonafied record of the work carried out under my supervision and guidance. It is further certified that no part of this thesis is submitted for the award of any degree.

Rourkela **(Dr. Dillip Ku. Bisoyi)**

Date - **Supervisor**

Department of Physics

ACKNOWLEDGEMENT

I express my sincere thanks to my supervisor, **Dr. Dillip Ku. Bisoyi**, Department of Physics, NIT Rourkela, for his esteemed supervision, incessant support, inspiration and constructive criticism throughout my project work.

I accord my thanks to Dr. S.K Pratihar, Department of Ceramic engineering, NIT Rourkela, for providing me with all necessary characterization facilities during the project work.

I would like to take the opportunity to thank Dr. U.K Mohanty, Department of MME, for allowing me to do SEM in his department. Also I thank Dr. S. Paria, Department of Chemical engineering, NIT Rourkela for permit me to use Particle size analyzer for my project work.

I would also thank to H.O.D and all my faculty members, office staffs and Technical staffs of Department of Physics , NIT Rourkela, for their co-operation.

I wish to extend my sincere thanks to Mr. Alok all for his help and moral support, without whom it couldn't be possible.

I convey my thanks to all my class mates, Miss. Annapurna Patra, Mr. Prakash, Mr. Naresh (PhD scholars) for their valuable suggestion and help.

Finally, I would also express my deep sense of gratitude to my parents and family members for their encouragement and support throughout, which always inspired me.

Rourkela **(Jayanta Kumar Behera)**

Date:

CONTENTS

List of Figures

ABSTRACT

The ZnO nanoparticles were prepared by two different methods where the size of the particles formed were found to be 320 nm and 559 nm studied by the particle size analyzer. The XRD patterns of these sample revealed that the required phase is present with a little amount of impurities. The particle size measurement which was done by particle analyzer was supported by the XRD Scherer's formula. SEM micrographs of ZnO-1 sample showed that agglomeration has been taken place where as in ZnO-2 sample showed no more agglomeration. EDX of the ZnO-1 sample confirmed the presence of both Zn and O. DSC analysis of the ZnO-1 sample ensured that there are two endothermic reactions have been taken place at temperature 135^0 C and 165^0 C but for ZnO-2 sample only one peak was found at 150^0 C which reveals that only one endothermic reaction has been taken place. Again TGA analysis of the samples showed significant weight loss of about 5% and 10% at 135^0 C and 165^0 C temperature respectively in case of ZnO-1 but the weight loss of about 10% has been found at 150^0 C temperature in case of ZnO-2 sample.

1. INTRODUCTION

Zinc oxide is an inorganic compound with the formula ZnO. It usually appears as a white powder, nearly insoluble in water. The powder is widely used as an additive into numerous materials and products including plastics, ceramics, glass, cement, rubber (e.g. car tyres), lubricants, paints, ointments, adhesives, sealants, pigments, foods (source of Zn nutrient), batteries, ferrites, fire retardants, etc. ZnO is present in the Earth crust as a mineral zincite; however, most ZnO used commercially is produced synthetically.

In materials science, ZnO is often called a II-VI semiconductor because zinc and oxygen belong to the 2nd and 6th groups of the periodic table, respectively. This semiconductor has several favorable properties: good transparency, high electron mobility, wide bandgap, strong room-temperature luminescence, etc. Those properties are already used in emerging applications for transparent electrodes in liquid crystal displays and in energy-saving or heat-protecting windows, and electronic applications of ZnO as thin-film transistor and light-emitting diode are forthcoming as of 2009.

CHEMICAL PROPERTIES

ZnO occurs as white powder commonly known as zinc white or as the mineral zincite. The mineral usually contains a certain amount of manganese and other elements and is of yellow to red color. Crystalline zinc oxide is thermo-chromic, changing from white to yellow when heated and in air reverting to white on cooling. This is caused by a very small loss of oxygen at high temperatures to form the non-stoichiometric $Zn_{1+x}O$, where at 800 °C, x= 0.00007.

Zinc oxide is an amphoteric oxide. It is nearly insoluble in water and alcohol, but it is soluble in (degraded by) most acids, such as hydrochloric acid:

$$ZnO + 2\ HCl \rightarrow ZnCl_2 + H_2O$$

Bases also degrade the solid to give soluble zincates:

$$ZnO + 2NaOH + H_2O \rightarrow Na_2(Zn(OH)_4)$$

ZnO reacts slowly with fatty acids in oils to produce the corresponding carboxylates, such as oleate or stearate. ZnO forms cement-like products when mixed with a strong aqueous solution of zinc chloride and these are best described as zinc hydroxy chlorides. This cement was used in dentistry.

ZnO also forms cement-like products when reacted with phosphoric acid, and this forms the basis of zinc phosphate cements used in dentistry. A major component of zinc phosphate cement produced by this reaction is hopeite, $Zn_3(PO_4)_2 \cdot 4H_2O$.

ZnO decomposes into zinc vapor and oxygen only at around 1975 °C, reflecting its considerable stability. Heating with carbon converts the oxide into zinc vapor:

$$ZnO + C \rightarrow Zn + CO$$

Zinc oxide reacts violently with aluminum and magnesium powders, with chlorinated rubber and linseed oil on heating causing fire and explosion hazard.

It reacts with hydrogen sulfide to give the sulfide: this reaction is used commercially in removing H_2S using ZnO powder (e.g., as deodorant).

$$ZnO + H_2S \rightarrow ZnS + H_2O$$

When ointments containing ZnO and water are melted and exposed to ultraviolet light, hydrogen peroxide is produced.

CRYSTAL STRUCTURES

Zinc oxide crystallizes in three forms: hexagonal wurtzite, cubic zincblende, and the rarely observed cubic rocksalt. The wurtzite structure is most stable and thus most common at ambient conditions. The zincblende form can be stabilized by growing ZnO on substrates with cubic lattice structure. In both cases, the zinc and oxide are tetrahedral. The rocksalt NaCl-type structure is only observed at relatively high pressures - ~10 GPa.

The hexagonal and zincblende ZnO lattices have no inversion symmetry (reflection of a crystal relatively any given point does not transform it into itself). This and other lattice symmetry properties result in piezoelectricity of the hexagonal and zinc blende ZnO, and in pyro-electricity of hexagonal ZnO.

The hexagonal structure has a point group 6 mm (Hermann-Mauguin notation) or C_{6v} (Schoenflies notation), and the space group is $P6_3mc$ or C_{6v}. The lattice constants are a = 3.25 Å and c = 5.2 Å; their ratio c/a ~ 1.60 is close to the ideal value for hexagonal cell c/a = 1.633. As in most II-VI materials, the bonding in ZnO is largely ionic, which explains its strong piezoelectricity. Due to this ionicity, zinc and oxygen planes bear electric charge (positive and negative, respectively). Therefore, to maintain electrical neutrality, those planes reconstruct at atomic level in most relative materials, but not in ZnO - its surfaces are atomically flat, stable and exhibit no reconstruction. This anomaly of ZnO is not fully explained yet.

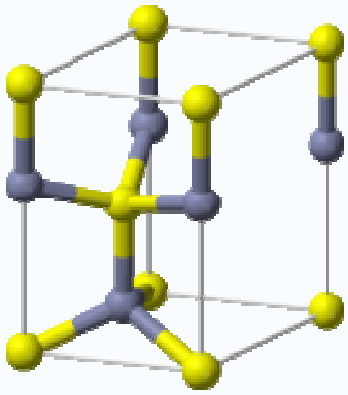

1. Wurtzite structure

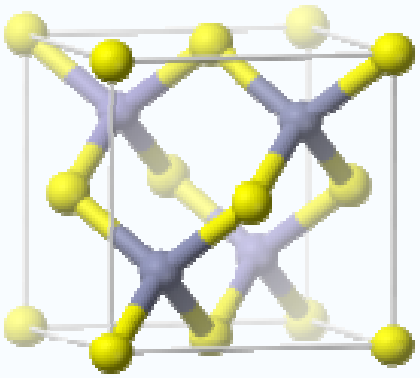

2. Zinc blende structure

Fig. 1 Crystal structures of ZnO

ELECTRONIC PROPERTIES

ZnO has a relatively large direct band gap of ~3.3 eV at room temperature; therefore, pure ZnO is colorless and transparent. Advantages associated with a large band gap include higher breakdown voltages, ability to sustain large electric fields, lower electronic noise, and high-

temperature and high-power operation. The bandgap of ZnO can further be tuned from ~3–4 eV by its alloying with magnesium oxide or cadmium oxide.

Most ZnO has *n*-type character, even in the absence of intentional doping. Native defects such as oxygen vacancies or zinc interstitials are often assumed to be the origin of this, but the subject remains controversial. An alternative explanation has been proposed, based on theoretical calculations, that unintentional substitutional hydrogen impurities are responsible. Controllable n-type doping is easily achieved by substituting Zn with group-III elements Al, Ga, In or by substituting oxygen with group-VII elements chlorine or iodine. Reliable p-type doping of ZnO remains difficult. This problem originates from low solubility of p-type dopants and their compensation by abundant n-type impurities, and it is pertinent not only to ZnO, but also to similar compounds GaN and ZnSe. Measurement of p-type in "intrinsically" n-type material is also not easy because inhomogeneity results in spurious signals.

Current absence of p-type ZnO does limit its electronic and optoelectronic applications which usually require junctions of n-type and p-type material. Known p-type dopants include group-I elements Li, Na, K; group-V elements N, P and As; as well as copper and silver. However, many of these form deep acceptors and do not produce significant p-type conduction at room temperature. Electron mobility of ZnO strongly varies with temperature and has a maximum of ~2000 $cm^2/(V \cdot s)$ at ~80 Kelvin.[21] Data on hole mobility are scarce with values in the range 5-30 $cm^2/(V \cdot s)$.

NANOTECHNOLOGY

The progress of technology and quality of life of mankind has always been closely knit with the progress in material science and material processing technology. Most material processing techniques are based on breaking up large chunk of a material into desired shapes and sizes, inducing strain, lattice defects and other deformations in the processed material. Recent developments in nanotechnology and the demonstration of various quantum size effects in nano-scale particles , implies that most of the novel devices of the future will be based on properties of nanomaterials . Each nanoparticle contains only about $3\text{-}10^7$ atoms/molecules. Lattice defects and

other imperfections induced by the traditional material processing techniques will no longer be diluted by sheer number of atoms, when used for synthesizing nanoparticles. Furthermore, it is difficult to achieve size selective synthesis of such small particles, by using the traditional approach.

Alternative synthetic technique for nanoparticles involves controlled precipitation of nanoparticles from precursors dissolved in a solution. A micro emulsion can also be formed between two immiscible liquids, using surfactants, with the reactants isolated inside a micelle, through hydrophobic versus hydrophilic forces. The resultant nanoparticles form a colloidal suspension. Various thermodynamic factors as well as van der Waal's forces induce particle growth and agglomeration , resulting in bigger particles that settle down over time. A prerequisite in utilizing colloidal nanoparticles is that they remain stable in colloidal suspension. Stabilization mechanism of nanoparticles can be categorized as a) electrostatic stabilization: involving the creation of a double layer of adsorbed ions over the nanoparticles resulting in a coulombic repulsion between approaching nanoparticles; or b) Steric hindrance: achieved by adsorption of polymer molecules over the nanoparticles. Osmotic repulsion felt by the polymer molecules due to localized increase in their concentration when polymer coated nanoparticles approach each other, keeps them (along with the nanoparticles) well separated.

2. LIRERATURE REVIEW

Zinc oxide (ZnO) is no stranger to scientific study. In the past 100 years, it has featured as subject of thousands of research papers, dating back as early as 1935 [1]. Valued for its ultra violet absorbance, wide chemistry, piezoelectricity and luminescence at high temperatures, ZnO has penetrated far into industry, and is one of the critical building blocks in todays modern society [2]. It can be found in paints, cosmetics, plastic and rubber manufacturing, electronics and pharmaceuticals, to name just a few. More recently however, ZnO has again entered the scientific spotlight, this time for its semiconducting properties [3]. Fueled out of advances in growth technologies and the potential for ZnO to become a suitable substrate for GaN, the fabrication of high quality single crystals and epitaxial layers was achieved [4, 5]. Allowing for the realisation of ZnO-based photonic and optoelectronic devices, where, amongst other potential applications it stands with GaN as a prospective candidate for the next generation of light emitters for solid state lighting applications [6, 7]. With a wide band gap of 3.4 eV and a large exciton binding energy of 60 meV at room temperature, ZnO holds excellent promise for blue and ultra-violet optical devices. Although in the past GaN and GaN-based materials have dominated this wavelength range, ZnO enters the arena with several advantages [3, 6]. The two most crucial of these are:

1. The larger exciton binding energy, which will allow for room temperature devices operating with higher efficiency and lower power threshold for lasing by optical pumping.
2. The ability to grow high quality single crystal substrates with relative cost effectiveness and ease - something that still eludes GaN Table 1.1 highlights some of the key properties of ZnO, and provides a comparison with GaN. Other favourable aspects of ZnO include its broad chemistry leading to many opportunities for wet chemical etching, piezoelectric properties, radiation hardness and high ferromagnetic Curie temperature for spintronic applications [8–11]. Together, these properties make ZnO an ideal candidate for a variety of devices including blue and ultra-violet laser diodes and light emitting diodes [12]. Despite the maturity of the field of semiconductors and the wide information base available for ZnO; as a semiconductor, little is actually known about this material. As with all wide band-gap semiconductors, ZnO has presented a number of hurdles to the scientific community which need to be understood and overcome before ZnO based devices can be commercially realised. The thesis come in what

could be described as the 'teenage years' of research into ZnO devices. The teething problems that initially hindered the realization of ZnO devices have been overcome. These would include mainly growth advances, which have seen the development of reproducible high quality epitaxial layers and single crystals [4, 5]. Zinc oxide (ZnO) is of great interest as a suitable material for high temperature, high power electronic devices either as the active material or as a suitable substrate for epitaxial growth of group III-nitride compound

UV photoconductivity of ZnO is governed by surface-related and bulk-related processes. The surface-related process is primarily governed by the adsorption and desorption of the chemisorbed oxygen at the surface of the ZnO, which is exploited for gas sensing applications [11]. This process becomes prominent in nanocrystalline films, where the surface area is large. In the bulk-related process, oxygen molecules in the grain boundaries contribute to photoconductivity. The bulk-related process is however considered to be faster in comparison to the surface-related process. For UV-detection, the fast component, due to the generation of photo carriers and their radiative and non-radiative recombination through local centres, is of greater importance [12]. Inherent defect centres, such as oxygen vacancies and zinc interstitials are believed to be responsible for visible photoluminescence in ZnO. Markevich et al. [13] have shown that recombination centers responsible for the orange band were the centers of photosensitivity. Defects in ZnO strongly depend on the preparation and annealing conditions which in turn affect the photoconduction properties. There have been studies on the effect of annealing under different conditions on the defect-related emission of ZnO thinfilms and nanostructures [14-17]. Thus Ghosh et al. [4] find that air-annealed ZnO films are preferable for photodetector applications due to the lower dark current. The large concentration of defects in the ZnO nanostructures prepared at low temperatures can be controlled by annealing in oxygen at different temperatures. It is therefore important to carry out a study of the

effect of annealing temperature on the photoluminescence as well as the photoconduction properties of ZnO nanostructures. In this communication, we report the effect of annealing in an oxygen atmosphere on the photoluminescence and photoconducting properties of thinfilms of colloidal ZnO nanoparticles.

3. SYNTHESIS OF MATERIALS

There are two method were used for the preparation of ZnO material, though there are several methods of preparation, as these method are easy with compared to other methods and the chemicals required for these methods are easily available and cheap.

SYNTHESIS OF ZnO-2

Zinc oxide was prepared from Zn nitrate solution after neutralizing with NaOH to pH values of 12. Conventional heating experiments were conducted on magnetic stirrer for experiment. When the reactions were completed, the solid and solution phases were separated by centrifugation and the solids were washed free of salts with de-ionized water (3X) and ethanol (2X). Then a white color powder was calcined at 80^0C and then grinded for uniformities of the powder. The dry synthetic powders were weighed and the percentage yields were calculated from the expected total amount of ZnO based on the solution concentration and volume and the amount that was actually crystallized.

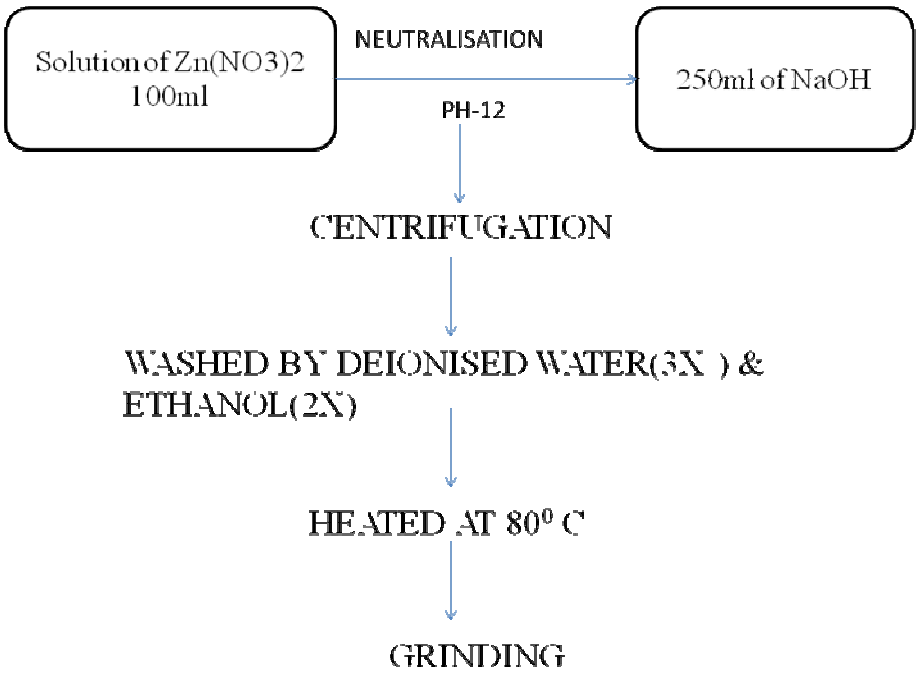

Fig. 2 Schematic diagram of synthesis of ZnO-2 sample

SYNTHESIS OF ZnO-1

The zinc oxide (ZnO) nanoparticles were prepared by wet chemical method using zinc nitrate and sodium hydroxides precursors and soluble starch as stabilizing agent. Different concentrations of soluble starch (0.1%), were dissolved in 500 ml of distilled water by using microwave oven. Zinc nitrate, 14.874 g (0.1 mol), was added in the above solution. Then the solution was kept under constant stirring using magnetic stirrer to completely dissolve the zinc nitrate for one hour. After complete dissolution of zinc nitrate, 0.2 mol of sodium hydroxide solution was added under constant stirring, drop by drop touching the walls of the vessel. The reaction was allowed to proceed for 2 h after complete addition of sodium hydroxide. After the completion of reaction, the solution was allowed to settle for overnight and the supernatant solution was then discarded carefully. The remaining solution was centrifuged at 10,000 ´ g for 10 min and the supernatant was discarded. Thus obtained nanoparticles were washed three times using distilled water. Washing was carried out to remove the byproducts and the excessive starch that were bound with the nanoparticles. After washing, the nanoparticles were dried at 80°C for overnight. During drying, complete conversion of Zn (OH)2 into ZnO takes place.

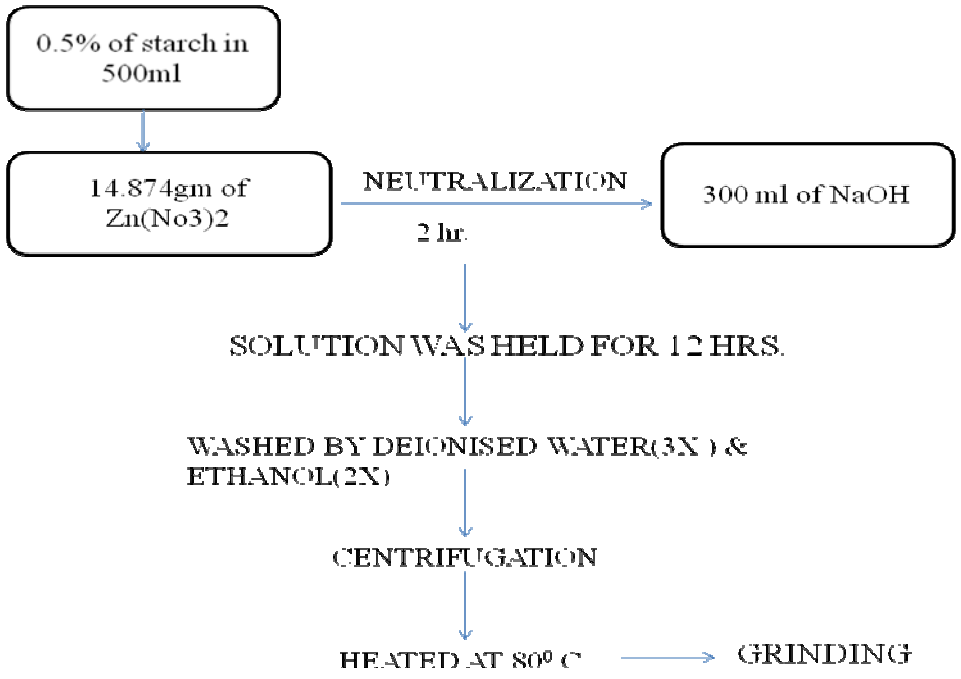

Fig. 3 Schematic diagram of synthesis of ZnO-1 sample

I.X-RAY Diffraction method

X-ray diffraction is a versatile, non-destructive analytical method for identification and quantitative determination of various crystalline forms, known as ‘phases’ of compound present in powder and solid samples. Diffraction occurs as waves interact with a regular structure whose repeat distance is about the same as the wavelength. The phenomenon is common in the natural world, and occurs across a broad range of scales. For example, light can be diffracted by a grating having scribed lines spaced on the order of a few thousand angstroms, about the wavelength of light. It happens that X-rays have wavelengths on the order of a few angstroms, the same as typical inter-atomic distances in crystalline solids. That means X-rays can be diffracted from minerals which, by definition, are crystalline and have regularly repeating atomic structures. When certain geometric requirements are met, X-rays scattered from a crystalline solid can constructively interfere, producing a diffracted beam. In 1912, W. L. Bragg recognized a predictable relationship among several factors.

1. The distance between similar atomic planes in a mineral (the interatomic spacing) which we call the d-spacing and measure in angstroms.

2. The angle of diffraction which we call the theta angle and measure in degrees. For practical reasons the diffractometer measures an angle twice that of the theta angle. Not surprisingly, we call the measured angle '2-theta'.

3. The wavelength of the incident X-radiation, symbolized by the Greek letter lambda and, in our case, equal to 1.54 angstroms.

$$n\lambda=2d\sin\theta ,$$

λ- wavelength of X-ray

d-interplaner spacing,

θ-diffraction angle

n-0,1,2,3….

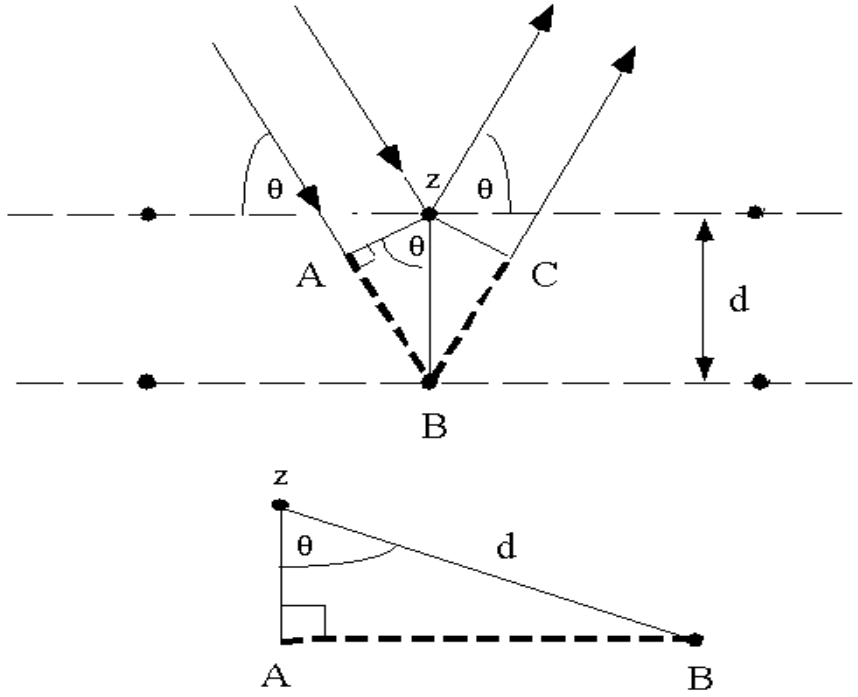

Fig. 4 Bragg's diffraction

Here XRD was done by the X-ray diffraction of the as milled powder samples were performed using the diffractometer. X-Ray diffraction patterns were recorded from 20˚ to 90˚ with a PANalytical system diffractometer (Model: DY-1656) using Cu K_α (λ=1.542A^o) with an accelerating voltage of 40 KV. Data were collected with a counting rate of 1˚/min. The K_α doublets were well resolved. From XRD, the crystallite size can be found out by using the scherrer's formula ,

$$P = \frac{0.9\lambda}{\beta \cos \theta}$$

Where

P – crystallite size

λ – wavelength(1.54A^0),

β - Full maxima half width,

θ- Diffraction angle

Fig.5 PANalytical system diffractometer (Model: DY-1656)

And by applying Scherer's formula, the crystallite size of the ZnO-1 and ZnO-2 sample found out to be approximately similar to the value measured by particle size analyzer. Here it is seen that the diffractograms are almost same but there are some undesired picks had been seen, due to the impurity phase present in the samples.

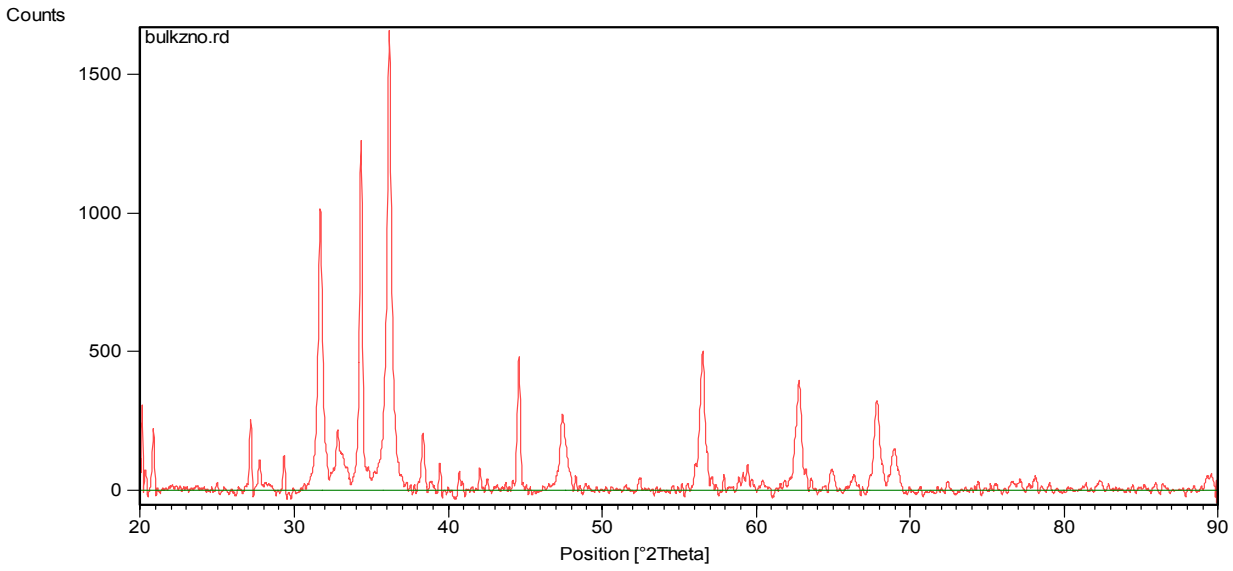

Fig. 6 XRD of ZnO-1

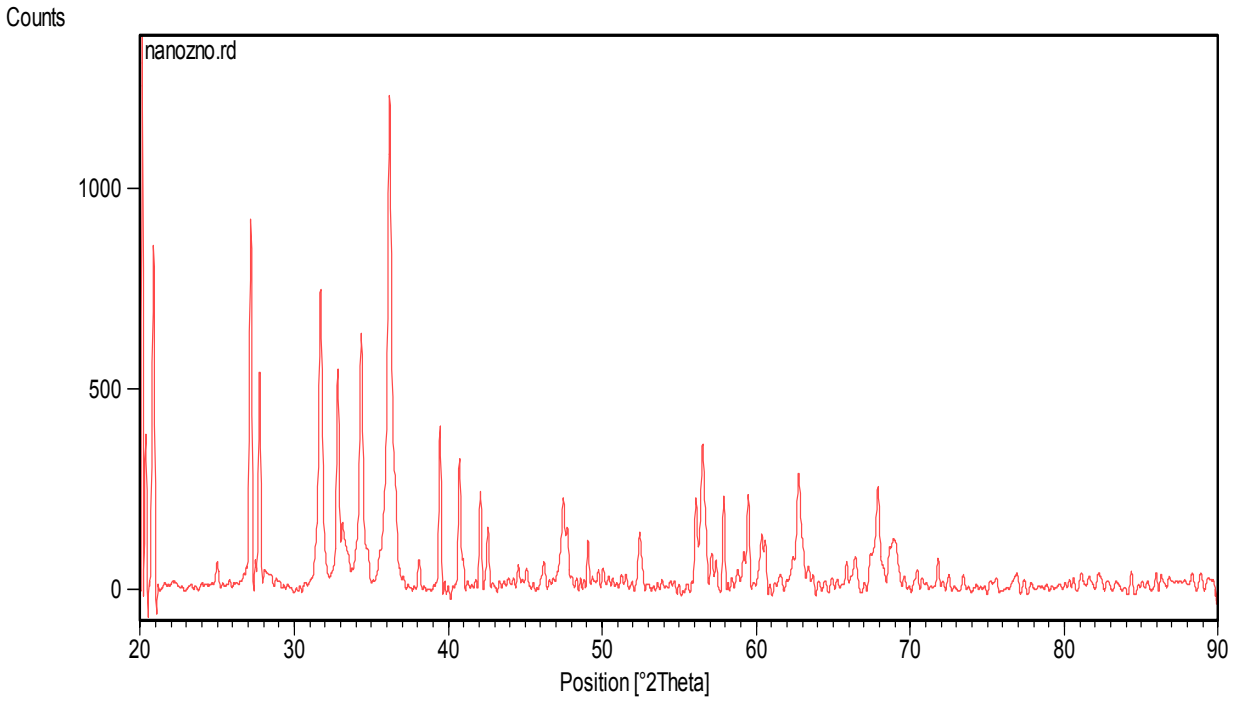

Fig. 7 XRD of ZnO-2

In both the figure represents the diffractogram of ZnO-1 and ZnO-2 samles, where both the highest pics were coming out at same angle 36.5^0. So from that one can roughly say that the sample were same.

II. **Scanning electron microscope (SEM)**

Fig. 8 SEM (JEOL-JSM 5800)

The scanning electron microscope (SEM) uses a focused beam of high-energy electrons to generate a variety of signals at the surface of solid specimens. The signals that derive from electron-sample interactions reveal information about the sample including external morphology (texture), chemical composition, and crystalline structure and orientation of materials making up the sample. In most applications, data are collected over a selected area of the surface of the sample, and a 2-dimensional image is generated that displays spatial variations in these properties. Areas ranging from approximately 1 cm to 5 microns in width can be imaged in a scanning mode using conventional SEM techniques (magnification ranging from 20X to approximately 30,000X, spatial resolution of 50 to 100 nm). The SEM is also capable of performing analyses of selected point locations on the sample; this approach is especially useful in qualitatively or semi-quantitatively determining chemical compositions (using EDS), crystalline structure, and crystal orientations (using EBSD). The design and function of the SEM is very similar to the EPMA, and considerable overlap in capabilities exists between the two instruments.

Fundamental Principles of Scanning Electron Microscopy (SEM)

Accelerated electrons in an SEM carry significant amounts of kinetic energy, and this energy is dissipated as a variety of signals produced by electron-sample interactions when the incident electrons are decelerated in the solid sample. These signals include secondary electrons (that produce SEM images), backscattered electrons (BSE), diffracted backscattered electrons (EBSD that are used to determine crystal structures and orientations of minerals), photons (characteristic X-rays that are used for elemental analysis and continuum X-rays), visible light (cathodoluminescence--CL), and heat. Secondary electrons and backscattered electrons are

commonly used for imaging samples: secondary electrons are most valuable for showing morphology and topography on samples and backscattered electrons are most valuable for illustrating contrasts in composition in multiphase samples (i.e. for rapid phase discrimination). X-ray generation is produced by inelastic collisions of the incident electrons with electrons in discrete ortitals (shells) of atoms in the sample. As the excited electrons return to lower energy states, they yield X-rays that are of a fixed wavelength (that is related to the difference in energy levels of electrons in different shells for a given element). Thus, characteristic X-rays are produced for each element in a mineral that is "excited" by the electron beam. SEM analysis is considered to be "non-destructive"; that is, x-rays generated by electron interactions do not lead to volume loss of the sample, so it is possible to analyze the same materials repeatedly.

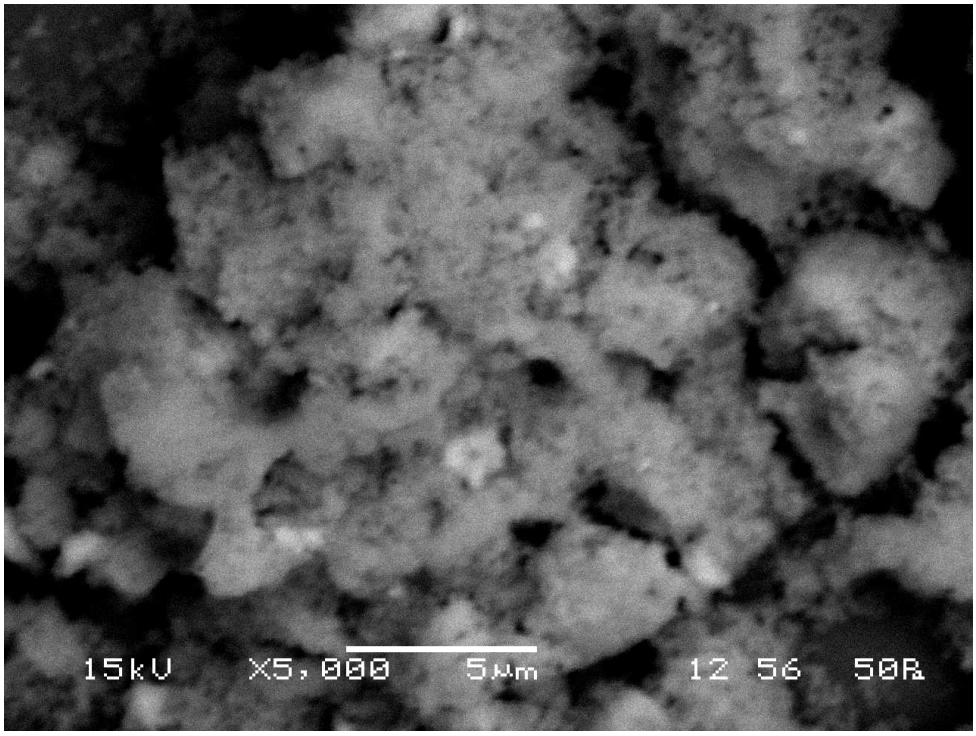

Fig. 9 SEM of ZnO-1

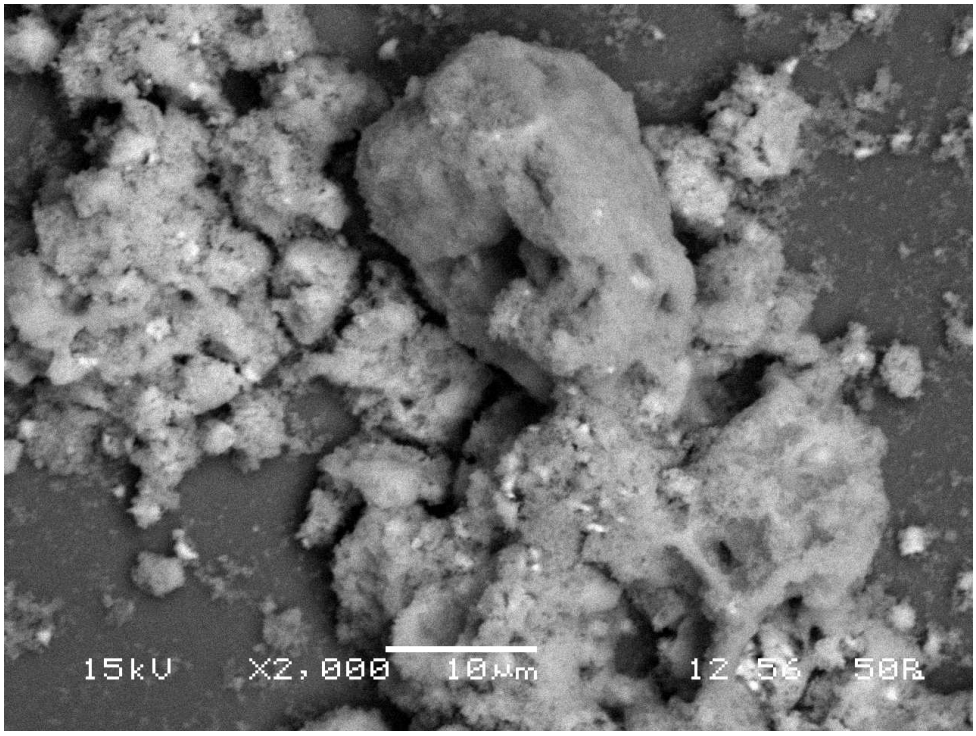

Fig. 10 SEM of ZnO-2

The SEM analysis of the ZnO-1 and ZnO-2 samples prepared from two different methods was done by SEM (JEOL-JSM 5800). The micrographs are shown above. Fig.- shows that a network formation of the ZnO-1 has taken place . It clearly indicates that agglomeration has taken place.

Similarly, in fig.- a big aggregation of the sample ZnO-2 particles has been taken place. It is not possible to predict the exact size of the individual particle, which can be done through TEM analysis. From the micrograph, it can be guessed that the particles are irregular in shape, but for the size of the particles, particle analyzer was done further.

III. Microscopic view

The optical microscope, often referred to as the "light microscope", is a type of microscope which uses visible light and a system of lenses to magnify images of small samples. Optical microscopes are the oldest and simplest of the microscopes. However, new designs of digital microscopes are now available which use a CCD camera to examine a sample and the image is shown directly on a computer screen without the need for expensive optics such as eye-pieces. Other microocopic methods which do not use visible light include scanning electron microscopy and transmission electron microscope. Here the microscopic view of the ZnO-2 is displayed below.

Here the microscopic view was taken by optical microscope with a magnification of 40X. At first the microscopic view of the powder was taken which is shown in the fig-_ and again the powder of Zno-2 sample was dispersed in water and the microscopic view was taken.

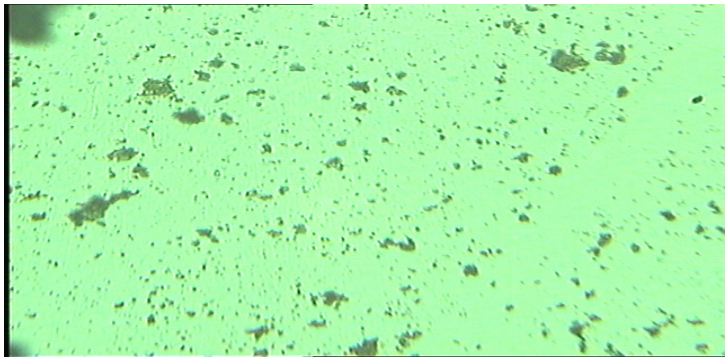

Fig. 11 Microscopic view of ZnO-2 in powder form

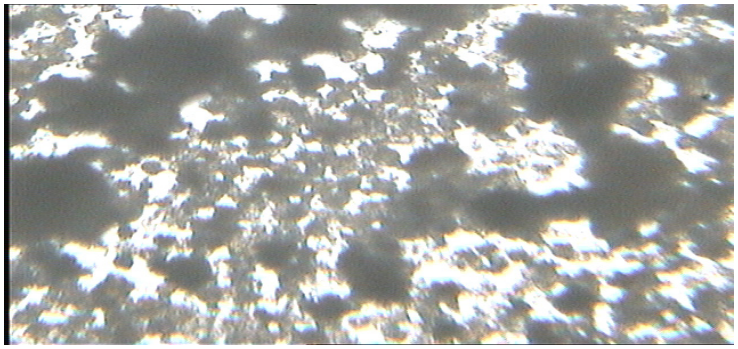

Fig. 12 Microscopic view of ZnO-2 in dispersed form

IV.Energy dispersive X-ray spectroscopy

Energy dispersive X-ray spectroscopy (EDS, EDX or EDXRF) is an analytical technique used for the elemental analysis or chemical characterization of a sample. It is one of the variants of XRF. As a type of spectroscopy, it relies on the investigation of a sample through interactions between electromagnetic radiation and matter, analyzing x-rays emitted by the matter in response to being hit with charged particles. Its characterization capabilities are due in large part to the fundamental principle that each element has a unique atomic structure allowing x-rays that are characteristic of an element's atomic structure to be identified uniquely from each other.

To stimulate the emission of characteristic X-rays from a specimen, a high energy beam of charged particles such as electrons or protons (see PIXE), or a beam of X-rays, is focused into the sample being studied. At rest, an atom within the sample contains ground state (or unexcited) electrons in discrete energy levels or electron shells bound to the nucleus. The incident beam may excite an electron in an inner shell, ejecting it from the shell while creating an electron hole where the electron was. An electron from an outer, higher-energy shell then fills the hole, and the difference in energy between the higher-energy shell and the lower energy shell may be released in the form of an X-ray. The number and energy of the X-rays emitted from a specimen can be measured by an energy dispersive spectrometer. As the energy of the X-rays are characteristic of the difference in energy between the two shells, and of the atomic structure of the element from which they were emitted, this allows the elemental composition of the specimen to be measured.

The excess energy of the electron that migrates to an inner shell to fill the newly-created hole can do more than emit an X-ray. Often, instead of X-ray emission, the excess energy is transferred to a third electron from a further outer shell, prompting its ejection. This ejected species is called an Auger electron, and the method for its analysis is known as Auger Electron Spectroscopy (AES).

X-ray Photoelectron Spectroscopy (XPS) is another close relative of EDS, utilizing ejected electrons in a manner similar to that of AES. Information on the quantity and kinetic energy of ejected electrons is used to determine the binding energy of these now-liberated electrons, which is element-specific and allows chemical characterization of a sample. EDS is often contrasted with its spectroscopic counterpart, WDS (Wavelength-Dispersive X-ray Spectroscopy). WDS

differs from EDS in that it uses the diffraction patterns created by light-matter interaction as its raw data. WDS has a much finer spectral resolution than EDS. WDS also avoids the problems associated with artifacts in EDS (false peaks, noise from the amplifiers and microphonics. In WDS only one element can be analyzed at a time, while EDS gathers a spectrum of all elements, within limits, of a sample.

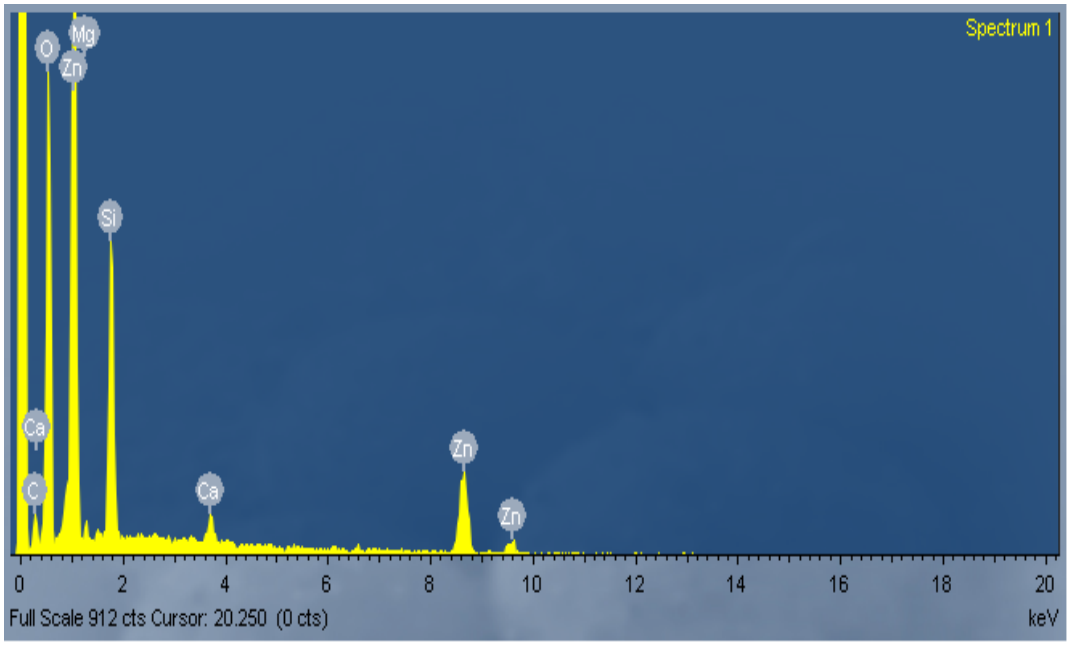

Fig. 13 EDX of ZnO-1

The EDX of the ZnO-1 sample was done by the SEM (JEOL-JSM 5800) machine . The EDX reveals that the required phase has present. Both Zinc(Zn) and Oxygen(o) is present in the sample . Again the graph shows the presence of Mg. and Si . This is due to the substrate over which it was held to do the SEM characterization.

V.PARTICLE SIZE ANLYZER

Particle size of the milled powder was measured by Malvern particle size analyzer (Model Micro-P, range 0.05-550 micron). Firstly, the liquid dispersant containing 500ml 0f distilled water and 25 ml of sodium hexa metaphosphate was kept in the sample holder. Then the instrument was run keeping ultrasonic displacement at 10.00 micron and pump speed 1800 rpm. A pinch of powders was added to the liquid dispersant so that the obscuration value varies between 10 to 30% and the residual below 1%.

Fig. 14 Malvern particle size analyzer (Model Micro-P, range 0.05-550 micron).

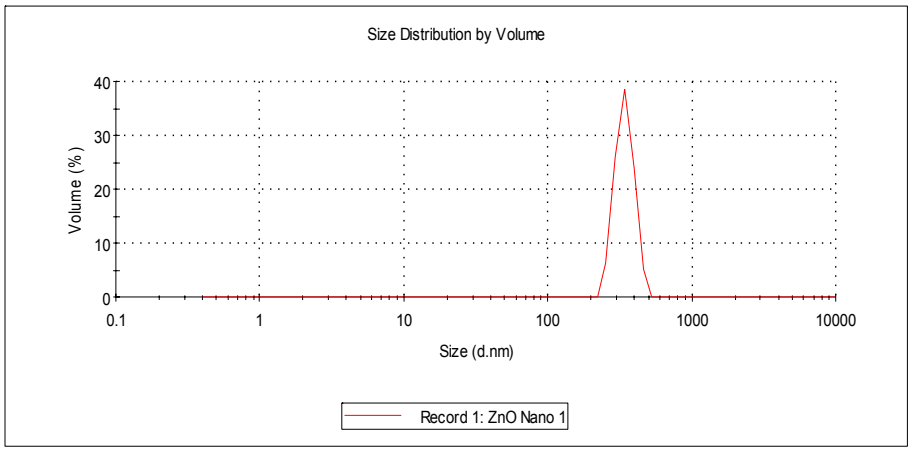

Fig. 15 Particle size of ZnO-1

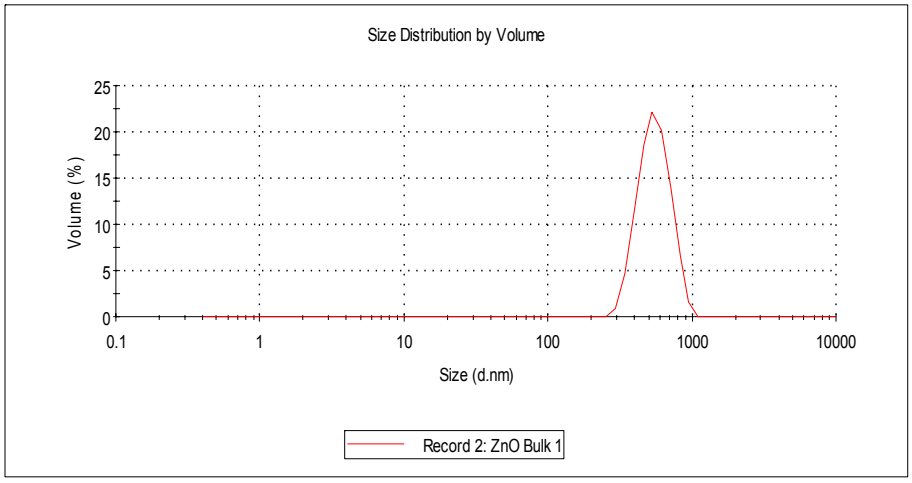

Fig. 16 Particle size of the ZnO-2

The above graphs showing the particle size of both the sample ZnO-1 and ZnO-2. After analyzing, it was found that the particle size of the ZnO-1 is 320 nm and particle size of the ZnO-2 is 559 nm.

VI.DSC Characterization

Differential scanning calorimetry or DSC is a thermo-analytical technique in which the difference in the amount of heat required to increase the temperature of a sample and reference are measured as a function of temperature. Both the sample and reference are maintained at nearly the same temperature throughout the experiment. Generally, the temperature program for a DSC analysis is designed such that the sample holder temperature increases linearly as a function of time. The reference sample should have a well-defined heat capacity over the range of temperatures to be scanned.

The main application of DSC is in studying phase transitions, such as melting, glass transitions, or exothermic decompositions. These transitions involve energy changes or heat capacity changes that can be detected by DSC with great sensitivity.

The technique was developed by E.S. Watson and M.J. O'Neill in 1960, and introduced commercially at the 1963 Pittsburgh Conference on Analytical Chemistry and Applied

Spectroscopy. The basic principle underlying this technique is that, when the sample undergoes a physical transformation such as phase transitions, more or less heat will need to flow to it than the reference to maintain both at the same temperature. Whether more or less heat must flow to the sample depends on whether the process is exothermic or endothermic. For example, as a solid sample melts to a liquid it will require more heat flowing to the sample to increase its temperature at the same rate as the reference. This is due to the absorption of heat by the sample as it undergoes the endothermic phase transition from solid to liquid. Likewise, as the sample undergoes exothermic processes (such as crystallization) less heat is required to raise the sample temperature. By observing the difference in heat flow between the sample and reference, differential scanning calorimeters are able to measure the amount of heat absorbed or released during such transitions. DSC may also be used to observe more subtle phase changes, such as glass transitions. DSC is widely used in industrial settings as a quality control instrument due to its applicability in evaluating sample purity and for studying polymer curing. Since DSC is more sensitive to phase transition temperature (with a precision of 0.01oC) and is capable of monitoring the exact rate of energy exchange or reaction rate. Positions of all these peaks depend on heating rate. Increasing the heating rate caused every peak shift toward higher temperatures, with the first two endothermic peaks merged into one broad one. This is due to activation energy involved in such transition.

Here the Differential Scanning Calorimetric analysis of the ZnO samples was done by heat-flux calorimeter 2920 DSC (Thermal Analysis Instruments, Inc.. Both sample showing different reactions were happened. In the ZnO-1 sample there are two picks are there at around 135^0 c and 165^0 c. Both are endothermic reactions. This is due to change of phases at that temperature.

Similarly in the ZnO-2 sample the only one pick has came at 150^0 c.

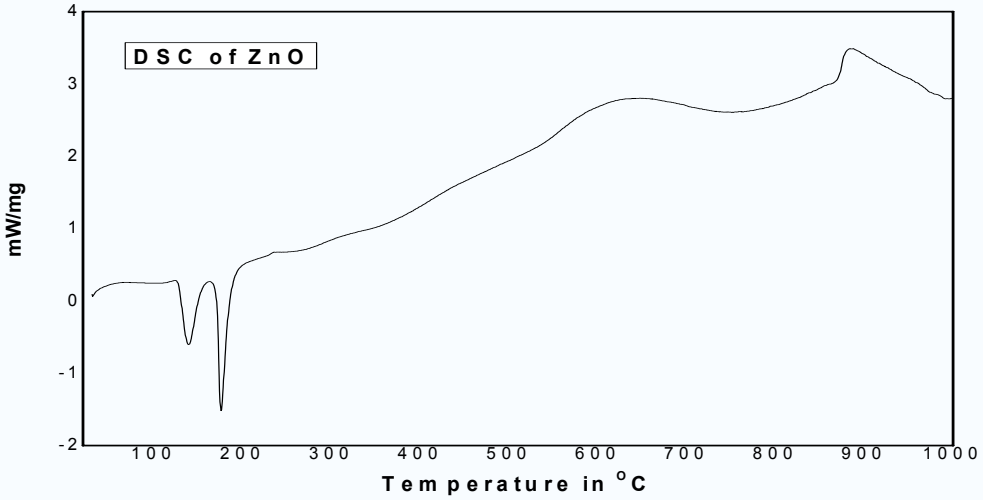

Fig.17 DSC analysis of ZnO-1

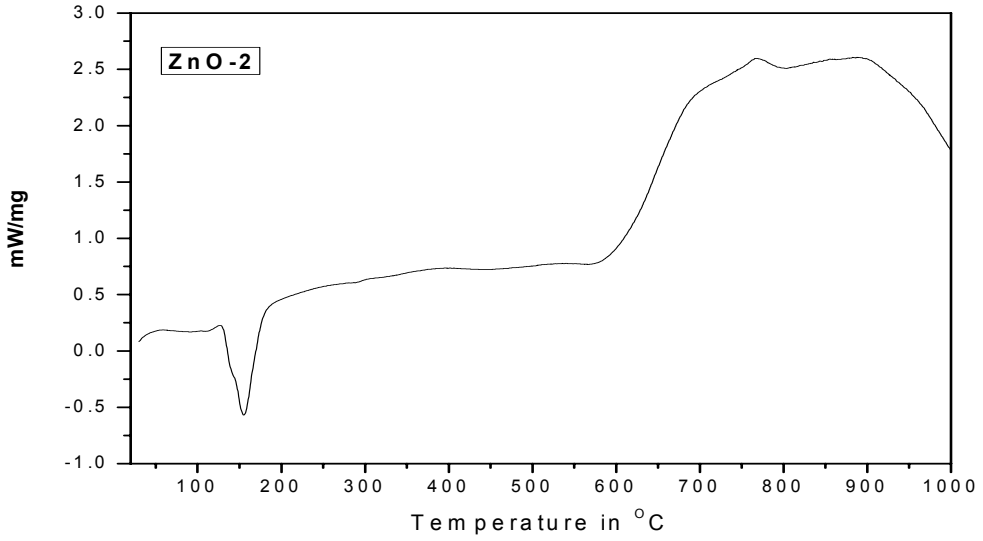

Fig. 18 DSC analysis of ZnO-2

VII.Thermo graviometric analysis

Thermograviometric Analysis or **TGA** is a type of testing that is performed on samples to determine changes in weight in relation to change in temperature. Such analysis relies on a high degree of precision in three measurements: weight, temperature, and temperature change. As many weight loss curves look similar, the weight loss curve may require transformation before results may be interpreted. A derivative weight loss curve can be used to tell the point at which weight loss is most apparent. Again, interpretation is limited without further modifications and deconvolution of the overlapping peaks may be required.

TGA is commonly employed in research and testing to determine characteristics of materials such as polymers, to determine degradation temperatures, absorbed moisture content of materials, the level of inorganic and organic components in materials, decomposition points of explosives, and solvent residues. It is also often used to estimate the corrosion kinetics in high temperature oxidation. The analyzer usually consists of a high-precision balance with a pan (generally platinum) loaded with the sample. The pan is placed in a small electrically heated oven with a thermocouple to accurately measure the temperature. The atmosphere may be purged with an inert gas to prevent oxidation or other undesired reactions. A computer is used to control the instrument.

Analysis is carried out by raising the temperature gradually and plotting weight against temperature. The temperature in many testing methods routinely reaches 1000°C or greater, but the oven is so greatly insulated that an operator would not be aware of any change in temperature even if standing directly in front of the device. After the data is obtained, curve smoothing and other operations may be done such as to find the exact points of inflection.

A method known as hi-res TGA is often employed to obtain greater accuracy in areas where the derivative curve peaks. In this method, temperature increase slows as weight loss increases. This is done so that the exact temperature at which a peak occurs can be more accurately identified. Several modern TGA devices can vent burnoff to a fourier-transform infrared spectrophotometer to analyze composition.

Here TGA analysis of the samples ZnO-1 and ZnO-2 were done by the instrument with a heatin rate of 1^0 C/min. The TGA graph of the sample ZnO-1 showing that a continues weight loss was happened up to 500^0 C, after that there is no significant loss of heat was observed. At 135^0 C and 165^0 C, sharp weight loss found.

Similarly, The TGA graph of ZnO-2 showing there is an only one sharp down fall which indicates that there at 150^0 C, a significant weight loss. though there is a continues weight loss was happened up to 700 ^{0}C. .

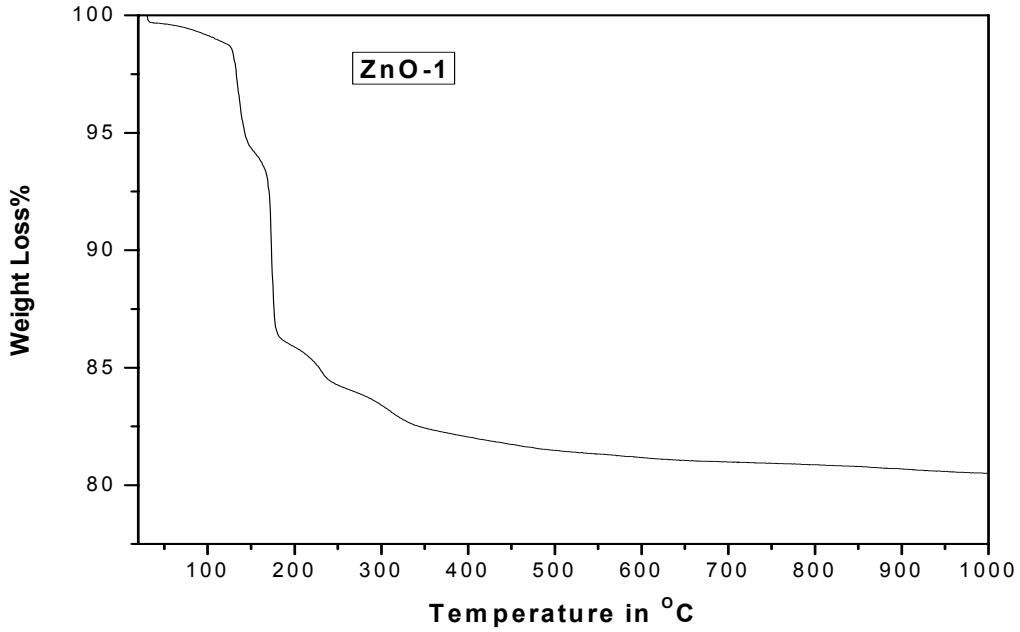

Fig.19 TGA analysis of ZnO-1

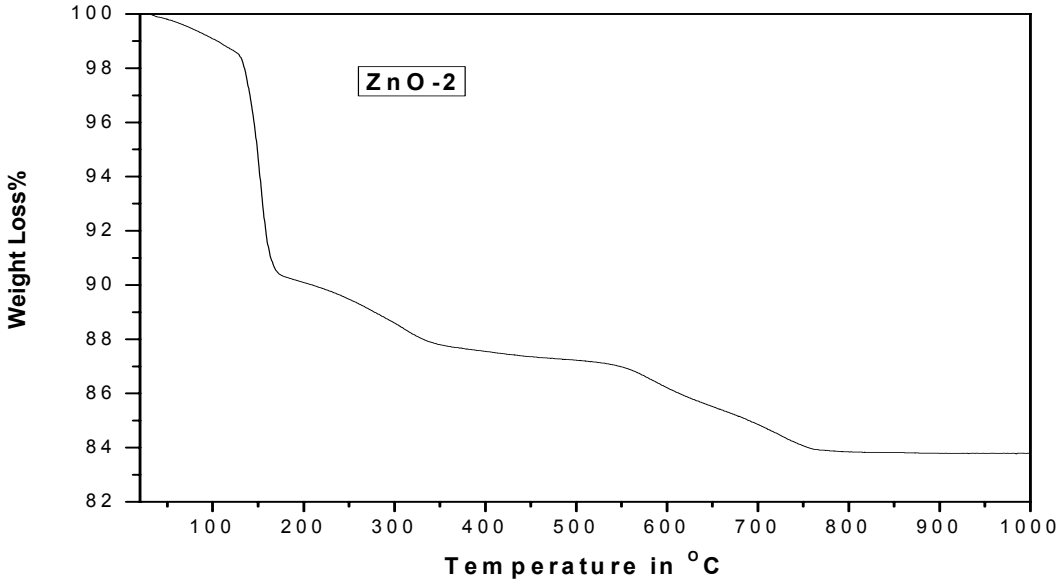

Fig.20 TGA analysis of ZnO-2

5. CONCLUSION

The ZnO nanoparticles were prepared by two different methods where the size of the particles formed were 320 nm and 559 nm studied by the particle size analyzer.

The XRD of these sample reveals that the required phase is present with a little amount of impurities. The particle sizes which was done by particle analyzer was supported by the XRD Scherer's formula.

SEM of the ZnO-1 sample showing that agglomeration has been taken place where as in ZnO-2 sample, it is not agglomerate. The particle size is irregular prepared from both the methods.

.EDX of the ZnO-1 sample showing both Zn and O present along with Mg and Si as the sample was held by a glass substrate for characterization.

DSC of the ZnO-1 ensures that there are two endothermic reactions have been taken place at temperature In the ZnO-1 sample there are two picks are there at around 135^0 c and 165^0 c. Both are endothermic reactions. This is due to change of phases at that temperature. But in the ZnO-2 sample the only one pick has came at 150^0 c.

TGA analysis of both the sample supports the results coming out from DSC analysis that the weight loss were seen at 135^0 C and 165^0 C in the ZnO-1 sample around 5% and 10% respectively and in case of ZnO-2 sample, the weight loss was about 10% at 150 ^{0}C . Though the samples were same but size were different, may be the cause of this type of different characteristics of the samples.

6. REFERENCE

1. C. W. Bunn, "The lattice-dimensions of zinc oxide," *Proc. Phys. Soc. London* **47**: 835,1935.

2. D. R. Lide (editor), *CRC Handbook of Chemistry and Physics*, CRC Press, New York, 73rd edition,
1992.

3. D. C. Look, "Recent advances in ZnO materials and devices," *Mat. Sci. Eng. B.* **80**: 383, 2001.

4. D. C. Look, D. C. Reynolds, J. R. Sizelove, R. L. Jones, C. W. Litton, G. Cantwell and W. C. Harsch,
"Electrical properties of bulk ZnO," *Solid State Commun.* **105**: 399, 1998.

5. Y. Segawa, A. Ohtomo, M. Kawasaki, H. Koinuma, Z. K. Tang, P. Yu and G. K. L. Wong,
"Growth of ZnO thin films by laser-MBE: Lasing of excitons at room temperature," *Phys. Stat. Sol.* **202**: 669, 1997.

6. J. E. Nause, "ZnO broadens the spectrum," *III-Vs Review* **12**: 28, 1999.

7. J. E. Nause, "Fluorescent substrate offers route to phosphor-free LEDs," *Comp. Semicond.* **11**: 29, 2005.

8. S. O. Kucheyev, J. S. Williams, C. Jagadish, J. Zou, C. Evans, A. J. Nelson and A. V.Hamza, "Ion-
beam-produced structural defects in ZnO," *Phys. Rev. B* **67**: 094 115, 2003.

9. C. Coskun, D. C. Look, G. C. Farlow and J. R. Sizelove, "Radiation hardness of ZnO at low temperatures," *Semicond. Sci. Technol.* **19**: 752, 2004.

10. S. O. Kucheyev, J. S. Williams and C. Jagadish, "Ion-beam-defect processes in group-III nitrides and ZnO," *Vacuum* **73**: 93, 2004.

11. N. A. Spaldin, “Search for Ferromagenetism in transition-metal-doped piezoelectric ZnO,” *Phys. Rev. B* **69**: 125 201, 2004.

12. S. J. Pearton, D. P. Norton, K. Ip, Y. Heo and T. Steiner, “Recent advances in processing of ZnO,” *J. Vac. Sci. Technol. B* **22**: 932, 2004.

13. D. C. Look and B. Claflin, “P-type doping and devices based on ZnO,” *Phys. Stat. Sol. (b)* **241**: 624, 2004.

14. D. C. Look, B. Claflin, Y. I. Alivov and S. J. Park, “The future of ZnO light emitters,” *Phys. Stat. Sol. (a)* **201**: 2203, 2004.

15. S. B. Zhang, S. H. Wei and A. Zunger, “Intrinsic *n*-type versus *p*-type doping asymmetry and the defect physics of ZnO,” *Phys. Rev. B* **63**: 075 205, 2001.

16. A. F. Kohan, G. Ceder, D. Morgan and C. G. Van deWalle, “First-principles study of native point defects in ZnO,” *Phys. Rev. B* **61**: 15 019, 2000.

17. C. G. Van de Walle, “Hydrogen as a cause of doping in ZnO,” *Phys. Rev. Lett.* **85**: 1012, 2000.